

Chlorine monoxide in the Antarctic spring vortex

2. A comparison of measured and modeled diurnal cycling over McMurdo Station, 1993

D. T. Shindell¹ and R. L. de Zafra²

Physics Department, State University of New York, Stony Brook

Abstract. We have derived chlorine monoxide (ClO) mixing ratio profiles within the Antarctic vortex on an hourly basis from ground-based measurements of pressure-broadened emission line spectra. This data set has provided the first opportunity for a detailed comparison between the output of a photochemical model and the measured in situ diurnal behavior of ClO in the Antarctic spring stratosphere. We stress the importance of the diurnal behavior in furnishing a short-term, crucial test of the catalytic chlorine chemistry which determines longer-term ozone depletion. We obtain excellent agreement between our measured and modeled diurnal change using the rate constants recommended in the 1994 Jet Propulsion Laboratory (JPL) evaluation, giving support to current understanding of perturbed chlorine chemistry in the Antarctic spring vortex. We have furthermore found that we can use our data to narrow the listed 1994 JPL uncertainty range for the ClO dimer formation rate constant and the equilibrium constant between ClO dimer formation and thermal dissociation. We show that the new limits we set on the dimer formation rate constant reduce the uncertainty in the daily rate of chlorine catalyzed ozone loss calculated from observed ClO concentrations by ~40% at 186-196 K. We find that a modeled total ozone loss rate including both chemistry and vertical transport, based on our measurements, agrees rather well with the amount and the linear trend of ozone loss seen throughout September in coincident balloon measurements.

Introduction

The majority of model studies of polar chlorine chemistry have dealt primarily with chemical trends taking place over periods of time from weeks to months, such as seasonal ozone loss [e.g., Lefèvre *et al.*, 1994; Rodriguez *et al.*, 1989]. Modeling of chemical processes which vary over shorter timescales can be used to probe other aspects of stratospheric chemistry, including the diurnal chlorine monoxide (ClO) dimer catalytic cycle of ozone destruction which is responsible for the majority of the annual Antarctic spring ozone depletion. Unfortunately, the lack of detailed diurnal data has until now prevented a detailed comparison of modeled and observed diurnal variation in the polar regions. We present here what we believe is the first such comparison.

In recent field campaigns at McMurdo Station, Antarctica, we have obtained a unique data set which shows diurnal variation of chlorine monoxide (ClO) within the polar vortex on an hourly basis. This has been made possible by use of a new receiver with improved sensitivity, which has decreased the time needed to acquire data with a given signal-to-noise ratio by nearly a factor of 4 relative to that used in our previous work [e.g., de Zafra *et al.*, 1989]. We have also developed a photochemical model specifically tailored to look at diurnal processes. A comparison of model predictions with data allows us to examine present understanding of chlorine catalytic chemistry by testing the ability of a model to reproduce the observed diurnal variation of ClO. This cycling of ClO through dimer formation and photolysis causes by far the most important catalytic destruction of O₃ in the Antarctic spring. Here, the extreme removal of NO_x typically leads to substantially greater peak values of ClO than in the Arctic, making the dimer cycle far more efficient than the BrO-ClO cycle. Thus, reproducing the measured short-term diurnal behavior of ClO provides a critical test of the mechanisms which are responsible for longer-term ozone depletion over Antarctica.

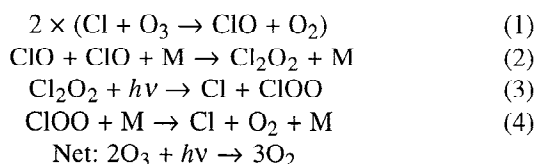
The chlorine monoxide dimer catalysis cycle [Molina and Molina, 1987], the primary cause of ozone depletion in the Antarctic lower stratosphere, is given by

¹Now at NASA Goddard Institute for Space Studies/Columbia University, New York.

²Also at Institute for Terrestrial and Planetary Atmospheres, State University of New York, Stony Brook.

Copyright 1996 by the American Geophysical Union.

Paper number 95JD03354.
0148-0227/96/95JD-03354\$05.00



At night, when there is no photolysis of the ClO dimer, the catalytic cycle does not take place, and ClO is partitioned between its monomer and dimer forms according to reaction (2), whose equilibrium point is temperature dependent, with the dominant form being the dimer in Antarctic spring conditions. In such conditions, the amount of ClO that takes part in other diurnal cycles, such as the chlorine nitrate cycle, is quite small. As the sun rises, the dimer is photolyzed, the ClO monomer builds up quickly, and reaction (2) in the forward direction becomes the rate limiting step for the catalytic cycle. We have observed, with good temporal resolution, the daily creation and destruction of a ClO layer in the lower stratosphere, and thus can directly examine the reaction rates of the chlorine catalytic cycle, the partitioning between chlorine species, and the resulting ozone depletion rates.

Diurnal Observations

We have measured ClO at McMurdo Station (77.8°S, 166.7°E) during the austral springs of 1986, 1987, 1992, and 1993, though we show 1993 data exclusively here and in *de Zafra et al.* [1995], a companion paper to this, since these data are the best taken to date. For the current work, a ground-based millimeter wave spectrometer employing a superconducting tunnel-junction detector for improved sensitivity was used [*de Zafra et al.*, 1994], allowing continuous observations of a full diurnal cycle at a single location with well-defined meteorological and photochemical conditions. Pressure-broadened emission spectra of the 278.63-GHz rotational transition of ClO were recorded. Data were grouped in 1-hour averages to improve the signal-to-noise ratio.

To remove a nearby ozone line, as well as weaker baseline artifacts in our signal, we have subtracted predawn spectra (measured within the same 24-hour time span) from all of our data, where predawn is defined as the last 4 hours before dawn. This differencing was carried out without "blanking and filling" of the narrow spectral region representing nighttime emission from high altitude ClO, in contrast with the procedure followed by *de Zafra et al.* [1995]. The differenced spectra dealt with here thus represent the hour by hour change of ClO at all altitudes, relative to its small predawn value. (Microwave Limb Sounder (MLS) measurements independently show that little lower stratospheric ClO remains by a few hours after sunset (J. Waters, personal communication, 1994).) We will restrict ourselves exclusively to diurnal variation below 30 km in the discussion which follows.

Our highest quality data were taken during early and mid-September. To improve the recovery of the time periods near sunrise and sunset, when the signal was

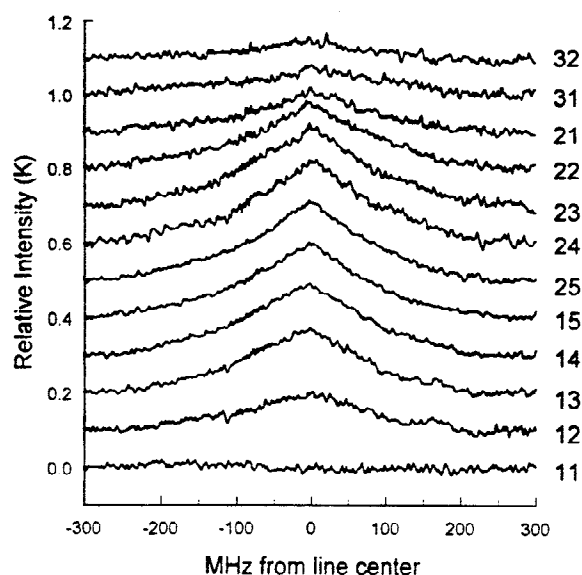


Figure 1. Diurnal variation in ClO emission spectra at 278,633 MHz observed from McMurdo Station, Antarctica, averaged over September 4-7, 1993. A predawn (4-0 hours before sunrise) spectrum has been subtracted from all of the spectra shown here to remove two nearby ozone lines and any baseline features within the handpass of our spectrometer. These differenced spectra thus represent the increase in the emission from its predawn value. The labels indicate the time of day in the form XY, where Y indicates the Yth hour, and X = 1, 2, and 3 indicate postsunrise, presunset, and postsunset, respectively. The ordinate gives intensity in terms of equivalent Rayleigh-Jeans emission temperature (K). The spectra have been offset by 0.1 K for clarity.

comparatively weak, we have averaged spectra together to form two representative time blocks, covering the periods September 4-7 and 17-20, during which times the amplitude of the midday signal was nearly constant. Given the considerable horizontal transport rates within the polar vortex, the relative consistency of our ClO measurements implies that chemical conditions for chlorine species were fairly homogeneous within the vortex air passing over McMurdo. Figure 1 presents the averaged differenced spectra in hourly intervals for the September 4-7 data (except for a 2-hour interval at midday). The spectra from both periods have been deconvolved to obtain vertical profiles of the diurnal change. The deconvolutions and error estimates were performed as described previously [*Shindell et al.*, 1994; *de Zafra et al.*, 1995]. Figure 2 shows the diurnal variation of ClO in hourly intervals (except during the essentially constant midday interval) averaged over September 4-7, 1993, as an example of recovered ClO profiles. Our midday profile agrees fairly well with MLS measurements of ClO (J. Waters, personal communication, 1994). This period, early September, is nearly coincident with the onset of the seasonal Antarctic "ozone hole" over McMurdo, as shown by balloon-borne ozonesondes [*Johnson et al.*, 1995].

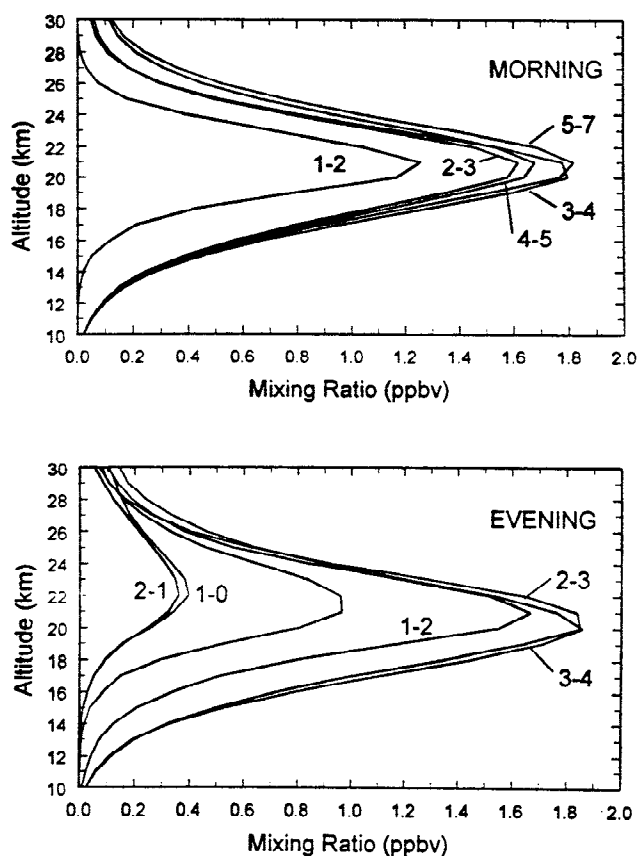


Figure 2. Diurnal variation of ClO in hourly intervals, except for a 2-hour period at midday. The “morning” panel shows vertical profiles averaged over the labeled hours after 20 km sunrise over McMurdo Station, Antarctica. All profiles in this panel except for the earliest one are within 1 sigma uncertainty of each other. The “evening” panel shows profiles averaged over the labeled hours before sunset at 20 km, except for the profiles labeled 1-0 and 2-1 which are from the periods 1 to 0 and 2 to 1 hours after sunset, respectively. Data have been averaged over September 4-7, 1993, and represent the increase from predawn mixing ratio.

Model Description

We have developed a detailed photochemical model focusing on the ability to accurately reproduce the rapid changes in the concentrations of trace species which occur near twilight. Special attention has been paid to the radiative transfer calculation and the initialization of molecular concentrations appropriate to the Antarctic spring, as well as to creation of a code which permits the use of very short chemical time steps.

During the period of maximum ozone destruction, when our observations were taken, the sun is at very high solar zenith angles. Therefore we have calculated the solar flux using a technique which is known to be accurate at very high angles, in the presence of a high polar surface albedo: we calculate the radiation field in a spherical atmosphere using tridiagonal matrix inversion [Toon *et al.*,

1989], and calculate the radiative transfer within each layer using the delta-Eddington method [Dvortsov *et al.*, 1992; Briegleb, 1992]. The model atmosphere runs from 0- to 60-km altitude, with 2-km intervals in the stratosphere and 1-km intervals in the troposphere. Photolysis rate constants are computed every 3 min for solar zenith angles less than 90° and every minute for angles between 90° and 97° . Scattered solar illumination is assumed to be zero for solar zenith angles greater than 97° . The solar flux at the top of the atmosphere is taken from a standard solar irradiance reference table for atmospheric modeling [World Meteorological Organization, 1985]. The surface albedo is set to 0.8. This value slightly influences the partitioning of chlorine, but the diurnal variation of ClO is very insensitive to this choice. For example, when the albedo is lowered from 0.8 to 0.2, much lower than we would expect to encounter in Antarctica during the early spring, the increase in ClO from its predawn value at 20-km altitude changes by less than 4% at any given time of day. Absorption due to molecular oxygen and ozone is calculated, with the ozone and pressure profiles taken from coincident balloon measurements performed at McMurdo Station by the University of Wyoming (B. Johnson, personal communication, 1993), supplemented by MLS ozone above 35 km altitude (J. Waters, personal communication, 1994).

In order to reduce computational time, the model assumes daytime photochemical equilibrium for five reactive families: HO_X (H, OH, and HO_2), O_X (O, O^1D , and O_3), NO_X (N, NO, NO_2 , and NO_3), Cl_X (Cl, ClO, and OClO), and Br_X (Br and BrO). This allows us to treat the extremely fast reactions between family members as only affecting the partitioning within the family. These intrafamily reactions (those reactions which cause no net change in the number of family molecules) are therefore independent of the time step chosen, which would otherwise have to be so short as to require prohibitively long computational times to simulate even a single day. However, we are concerned with photochemistry during periods of rapidly changing solar exposure near sunrise and sunset, which lead to rapid changes in the concentrations of trace species. By simulating one or at most a few days only, we are able to run the model efficiently with a time step of 30 s, which is short enough to accurately reproduce the diurnal variation of all trace species in the model. The model calculates the explicit solution of the differential equations for each species at every time step.

Initial molecular fields are based on data from a number of sources. The Wyoming balloon data mentioned previously are used for ozone. Our own midday-minus-predawn measurements are used to initialize midday ClO, with the addition of a small, calculated predawn residual amount of ClO (~ 0.1 ppbv using the recommended rate constants and photolysis cross sections given in the JPL 1994 evaluation [DeMore *et al.*, 1994, hereafter JPL 94]) whose abundance is in rough agreement with the nighttime ClO observations of the MLS given their fairly large uncertainties (J. Waters, personal communication, 1994).

Table 1. Initial Values at 20-km Altitude

Species	Mixing Ratio, ppbv	Species	Mixing Ratio
ClO	1.9	O ₃	1.7 ppmv
Cl ₂ O ₂	0.6	HNO ₃	1.3 ppbv
HCl	0.0	H ₂ O	2.5 ppmv
ClONO ₂	0.0	CH ₄	0.7 ppmv
HOCl	0.0	BrO	7.0 pptv
Cl _y	3.1		

Values for Cl₂O₂ and nighttime residual ClO (0.1 ppbv) were calculated using the ClO dimer reaction rates and photolysis cross sections recommended in the JPL 94 evaluation.

The model then calculates the amount of ClO dimer in midday equilibrium with ClO, which is a function of the ClO dimer formation rate, thermal dissociation rate, and photolysis rate. We find that 0.6 ppbv Cl₂O₂ is present at midday using the recommended rate constants and photolysis cross sections given in JPL 94. Combined with the 1.9 ppbv ClO from our observations (including the 0.1 ppbv nighttime residual), this gives 3.1 ppbv chlorine in ClO and its dimer, indicating roughly complete activation of chlorine.

Lidar measurements from McMurdo during 1993 showed the presence of polar stratospheric clouds (PSCs) around 20-km altitude in July and early August (A. Adriani, personal communication, 1994). Given that the conversion time of ClONO₂ and HOCl into active chlorine in the presence of large PSCs is only a few hours [Turco *et al.*, 1989], we assume that all ClONO₂ and HOCl has been depleted by early September through heterogeneous reactions with HCl on PSC surfaces, as per Crutzen *et al.* [1992]. The amount of HCl at 20-km altitude is set to 0.0 ppbv as well, given that nearly all available chlorine is contained in the reactive forms ClO and Cl₂O₂. Indeed, only very small abundances (~0.2 ppbv) of HCl were seen by the Halogen Occultation Experiment (HALOE) in late September 1993, when its field of observations first penetrated the polar vortex (J. Russell, personal communication, 1995). We have used HNO₃ values near the minimum seen by the Cryogenic Limb Etalon Array Spectrometer (CLAES) during September 1992, version 7 processing (J. Mergenthaler, personal communication, 1994) to represent conditions inside the southern hemisphere polar vortex after heterogeneous conversion of chlorine into active forms has taken place, and the lower stratosphere has been at least partially denoxified. Initial BrO values are extrapolated from aircraft measurements over Antarctica [Brune *et al.*, 1989].

Profiles for longer lived species are taken from three instruments aboard the Upper Atmospheric Research Satellite (UARS): We use CLAES version 7 observations of N₂O from September 1992, and HALOE version 17 observations of H₂O and CH₄ from October 1993 (J.

Russell, personal communication, 1995), both taken within the polar vortex near the latitude of McMurdo Station. CO₂ is initialized at a uniform mixing ratio of 350 ppmv at all altitudes [World Meteorological Organization, 1985], while the initial CO is set to that seen by the Improved Stratospheric And Mesospheric Sounder (ISAMS) instrument aboard UARS [López-Valverde *et al.*, 1993]. Table 1 summarizes the initial values at 20-km altitude for the species which are the most important in this study.

To initialize a number of other species in equilibrium with the species listed above, the model is run repeatedly through the same 24 hour cycle of illumination, with the data fields listed above reset to the original starting values every 24 hours, until each of the following species shows no further change at the end of a cycle relative to its beginning: Cl₂, HO₂NO₂, H₂O₂, N₂O₅, NO₂, HOCl, HBr, HOBr, BrCl, BrONO₂, CH₃O₂, CH₂O, ClONO₂, and H₂. This technique is used, instead of simply running at a fixed solar zenith angle, to obtain accurate fields for species such as N₂O₅ which are not in midday photochemical equilibrium.

We have used a fairly complete set of chemical reactions in our model to be sure that we have included all reactions of potential importance to the diurnal variation of chlorine monoxide, as well as to allow the model to be used in the future to explore such issues as the partitioning of chlorine between various species throughout the stratosphere and the diurnal variation of ClO in the polar upper stratosphere and at midlatitudes. The 39 molecules contained in the model interact via the 100 chemical and 31 photolytic reactions given in the appendix. For comparison, we note that the reaction list includes all of the reactions used by Lefèvre *et al.* [1994]. Chlorofluorocarbons (CFCs) have not been included in the model since their lifetimes are much longer than the period of a single day that we wish to examine. Heterogeneous reactions on nitric acid trihydrate (NAT) PSCs, reactions (96)-(100), and on liquid sulfate aerosols, reactions (96) and (97) only, have been included using the reaction probabilities on NAT and sulfate aerosol surfaces given in the JPL 1994 evaluation. The NAT surface area has been set to a constant, relatively small value (2 μm²/cm³) when temperatures are below 195 K, as limited PSCs were seen above 16 km in September 1993 observations from McMurdo [Johnson *et al.*, 1995]. The sulfate aerosol surface area profile is set to the mean value of September 1989 measurements at McMurdo Station [Hofmann and Deshler, 1991]. Type II water-ice PSCs are not included, as temperatures were too high for their presence during September 1993 over McMurdo.

Reaction rate constants and photolysis cross sections are taken from the JPL 94 evaluation with several exceptions noted at the end of the reaction lists given in the appendix. Atmospheric temperature and pressure profiles are taken from concurrent University of Wyoming ozonesondes up to ~35 km, and from National Meteorological Center data at higher altitudes.

Analysis

Sensitivity of Model Results

In Figure 3 we show the modeled mixing ratio versus time throughout September 6, 1993, for the most abundant chlorine species in the model: ClO and Cl₂O₂. All other chlorine species have a mixing ratio below 0.05 ppbv at all times. Clearly, it is the day-night cycling between the ClO monomer and the ClO dimer (reactions (1)-(4) above) which is responsible for the diurnal variation in ClO at 20 km. This situation is particular to the heterogeneously processed, denoxified lower stratosphere which exists during the Antarctic polar spring.

Since the diurnal variation of ClO is essentially a function of cycling between ClO and Cl₂O₂, changes within present uncertainties in the concentrations of other species and in other photochemical reactions have a minimal effect on our model/data comparison of the diurnal behavior of ClO. Though our model contains a rather large set of reactions, its output, not surprisingly, indicates that only those few reactions involving the ClO dimer catalytic cycle are important in determining the diurnal variation of ClO in the Antarctic lower stratosphere during early to mid September. Our model/data comparison is therefore a direct test of the validity of the JPL 94 recommended rate constants that govern the ClO dimer catalytic cycle.

Comparison Between Model and Data

We have compared our observations with the modeled diurnal variation of ClO when the rate constants and photolysis cross sections given in the JPL 94 recommendation are used. Our measurements from the 4-day period of September 4-7 have been compared with the

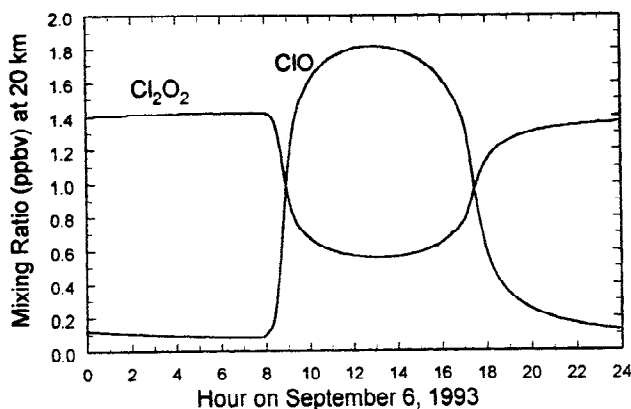


Figure 3. Modeled diurnal variation on September 6, 1993, at 20-km altitude over McMurdo Station, Antarctica. The most abundant chlorine-containing species, ClO and Cl₂O₂, are shown. All others have mixing ratios less than 0.05 ppbv at all times. Cycling between the ClO monomer and dimer accounts for nearly all of the diurnal variation in ClO under these polar spring conditions.

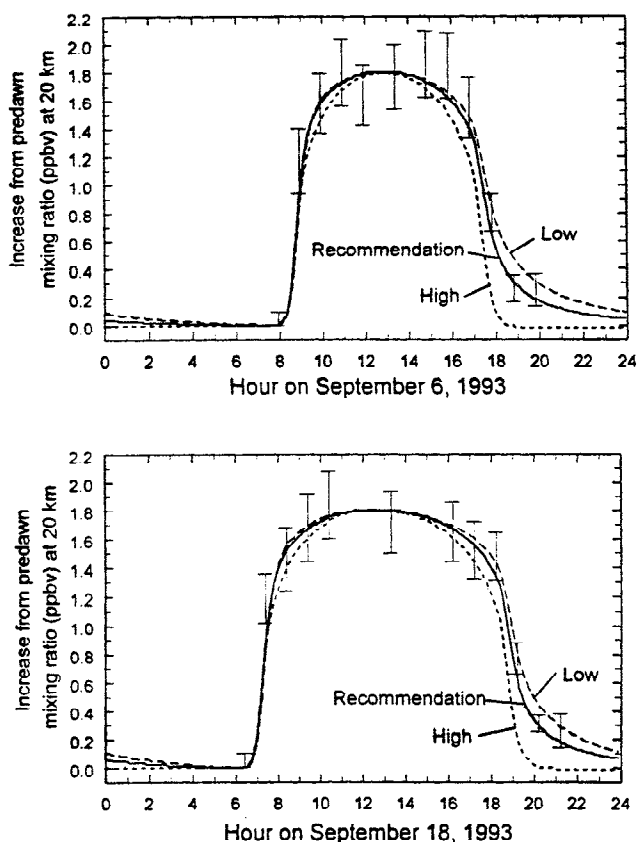


Figure 4. Modeled diurnal cycles of ClO at 20 km on September 6 and 18, 1993, versus measured ClO from September 4-7 and 17-20, 1993, respectively. Vertical error bars represent 1-sigma uncertainty in the observed increase from predawn mixing ratio. Curves are model results using the lower limit, recommended value, and upper limit for the ClO dimer thermal dissociation rate constant from the JPL 94 evaluation (see text). At 20 km, sunrise is at 7:25 and sunset is at 18:20 on September 6, while sunrise is at 5:55 and sunset is at 19:40 on September 18.

model day September 6, while our measurements from September 17-20 have been compared with the model day September 18. We have found excellent agreement between our observed record of diurnal change in ClO and that predicted by the model. The results are shown in Figure 4 for 20 km, approximately the altitude of the peak mixing ratio of ClO during September 4-7. The vertical error bars in Figure 4 represent the one-sigma uncertainty in the observed increase from predawn mixing ratios of ClO at 1-hour intervals (except for longer intervals at midday) starting at sunrise and continuing through the period 1-2 hours after sunset. The solid curves labeled "Recommendation" are the modeled diurnal variation of ClO, also shown as an increase from predawn values. The close agreement between the data and the model output suggests that the rate constants governing the ozone depleting ClO dimer catalytic cycle given in the 1994 JPL recommendation are essentially correct.

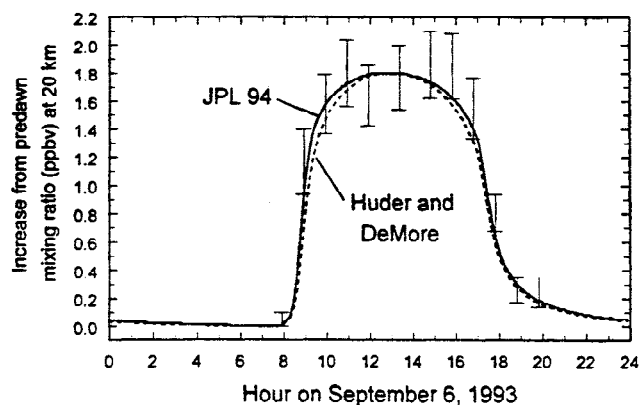


Figure 5. Modeled diurnal variation of ClO on September 6, 1993 at 20 km altitude over McMurdo Station, Antarctica. The two curves show the limited effect of even a fairly large variation in the photolysis cross sections of Cl_2O_2 . The JPL 94 evaluation values were used for the solid curve, while the smaller cross sections recently measured by *Huder and DeMore* [1995] were used for the dashed curve.

Constraints

Since the rates of reactions (1) and (4) in the ClO dimer catalytic cycle (see introduction section) are orders of magnitude faster than reactions (2) and (3), our results are only sensitive to the uncertainties in the rate limiting reactions (2) and (3): the ClO dimer formation rate, thermal dissociation rate, and photolysis rate. To establish constraints on these rates, we first examine the model's sensitivity to the ClO dimer photolysis cross sections.

The JPL 94 recommendations for the ClO dimer photolysis cross sections are the average of four sets of laboratory measurements up to 360 nm, with an extrapolated exponential curve at longer wavelengths. The four data sets agree within 10% at the cross-section maximum (245 nm), but disagree significantly at the longer wavelengths (>300 nm) where the majority of ClO dimer photolysis in the lower stratosphere takes place in our model. Recent measurements of *Huder and DeMore* [1995] give substantially smaller Cl_2O_2 cross sections in this longer wavelength region, leading to a midday photolysis rate (solar zenith angle 85°) on September 6, 1993, at 20 km of $J_{\text{Cl}_2\text{O}_2} = 5.4 \times 10^{-4} \text{ s}^{-1}$, only 55% of the rate we calculate using the JPL 94 cross sections, $J_{\text{Cl}_2\text{O}_2} = 9.6 \times 10^{-4} \text{ s}^{-1}$. Model results using both the JPL 94 recommendations and the new measurements of Huder and DeMore are shown in Figure 5. Clearly the shape of the curve is quite similar for the two cases, with the largest differences in early morning and late afternoon as expected. Given the large difference between the two sets of cross sections, these results indicate that the modeled diurnal change in ClO is fairly insensitive to the dimer photolysis cross section. The Cl_2O_2 cross sections do affect the partitioning of chlorine, however, since the equilibrium between ClO and Cl_2O_2 is quite different for the two cases.

At midday, when there is 1.9 ppbv ClO, there is 0.6 ppbv Cl_2O_2 using the JPL 94 photolysis cross sections, and 1.0 ppbv using the cross sections of Huder and DeMore. We will discuss this point further in the chlorine partitioning section of this paper.

The insensitivity of ClO diurnal behavior to the dimer photolysis cross sections leaves the modeled diurnal variation sensitive almost solely to the ClO dimer formation and thermal dissociation rates. The JPL evaluation data consist of the dimer formation rate constant and the equilibrium constant between dimer formation and thermal dissociation. We have compared our data to the model behavior when the thermal dissociation rate constant is varied to the limits allowed by the uncertainties quoted in JPL 94, since the uncertainty in this rate constant encompasses the uncertainties in both the formation rate constant and the equilibrium constant. The thermal dissociation rate constant is equal to the ratio of the formation rate constant to the equilibrium constant, and thus the low (high) dissociation rate constant is the ratio of the formation rate constant minus (plus) its uncertainty and the equilibrium constant plus (minus) its uncertainty. The results are shown in Figure 4 over a full diurnal cycle on September 6 and 18, 1993, at 20-km altitude. Since our midday observations were used to initialize the model, it is no surprise that all of the model runs agree at midday. However, there is a clearly a large difference in the rate at which ClO goes back into Cl_2O_2 near sunset using the different ClO dimer thermal dissociation rate constants.

It is revealing to compare our measurements with the model output at other altitudes as well. In Figure 6 we show ClO throughout the lower stratosphere for the time periods 1-0 hours before sunset at 20 km and 1-2 hours after sunset at 20 km. The profiles retrieved from our observations are shown, with uncertainties lying within the envelope of horizontal bars. For this analysis, we have imposed a relatively conservative cutoff of profile retrieval at 17 km, set by the bandpass of our spectrometer.

Though the results are clearly sensitive to the dimer thermal dissociation rate constant (the ratio of the dimer formation rate constant to the equilibrium constant), the influence of changing the formation rate constant or the equilibrium constant individually is not equivalent. The diurnal variation of ClO is determined by the complex balance between ClO dimer formation, thermal dissociation, and the changing amount of dimer photolysis. Therefore we have used the model to determine the individual contributions of the uncertainties in the dimer formation rate constant and the equilibrium constant. We have examined the variation in the dimer formation rate constant which maintains agreement with the data uncertainties when the equilibrium constant is also varied within the uncertainty given in JPL 94. This is in effect similar to adding the various sources of error, the measurement and equilibrium constant uncertainties, to determine the total error in the dimer formation rate constant. Our results apply to temperatures from ~ 186 -196

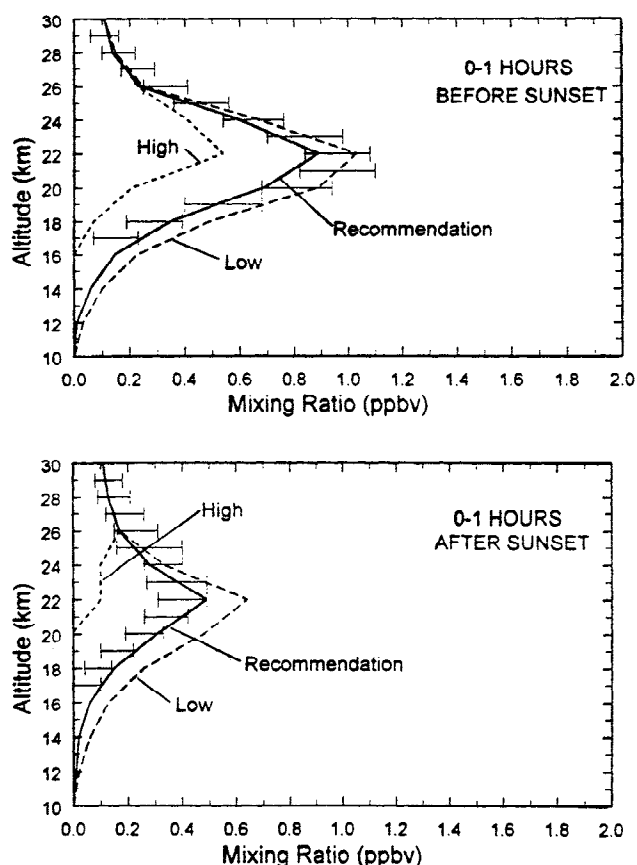


Figure 6. Comparison of measured and modeled vertical profiles for the periods 1-0 hours before sunset and 0-1 hours after sunset. The curves again show model behavior using the lower limit, recommended value, and upper limit for the ClO dimer thermal dissociation rate constant as given in the 1994 JPL evaluation.

K which were found in the lower stratosphere over McMurdo during early to mid-September.

We find that ClO dimer formation rate constant (R_2) must be no less than 0.7, nor greater than 1.3 times the JPL 94 recommendation, or agreement cannot be maintained within the 1-sigma uncertainty limits of our measurements, for any value of the equilibrium constant within its uncertainty as given in JPL 94. These limits on the ClO dimer formation rate constant amount to a

reduction of ~40% from the JPL 94 uncertainty range at 190 K.

Similarly, we also find that an equilibrium constant of less than 0.15 or greater than 26 times the JPL 94 recommendation does not maintain agreement with the 1-sigma uncertainty of our measurements for any value of the dimer formation rate constant within its uncertainty as given in JPL 94. This is a reduction of ~60% from the JPL 94 uncertainty range at 190 K. These results are summarized in Tables 2 and 3. For completeness, we also show actual laboratory measurements in these tables, and we point out that the uncertainty ranges established in our model/measurement comparison are quantitatively similar to those established in the laboratory. Since we are concerned with the suitability of reaction rates for atmospheric modeling however, we have confined our uncertainty comparison to the JPL 94 evaluation, the standard reference for modeling.

Chlorine Partitioning

The total amount of inorganic chlorine which is present under a given partitioning is an additional constraint on the allowed reaction rates. ClO is initialized by means of our observed predawn to midday increase in concentration. As mentioned above, the model adds in the calculated nighttime amount of ClO to obtain the total midday concentration of ClO which yields the observed midday-minus-predawn increase at the specified reaction rates. The amount of Cl_2O_2 , as well as other trace species, in equilibrium with the monomer and the other initial concentrations at all altitudes is then calculated.

The mixing ratios of ClO and Cl_2O_2 at 20 km altitude calculated using the JPL 94 recommendations were shown in Table 1. In Table 4 we show the amount of chlorine in ClO, Cl_2O_2 , and the total amount required in both species ($\text{ClO} + 2 \times \text{Cl}_2\text{O}_2$) as the ClO dimer reaction rate constants and photolysis cross sections are varied as outlined above. There was assumed to be a total of 3.8 ppbv total chlorine loading in the troposphere in 1989, increasing at 2.8%/year [World Meteorological Organization, 1991]. Based on a 5-year age for polar stratospheric air [Schmidt and Khedim, 1991; J. S. Daniel, personal communication, 1995], the total loading in the 1993 Antarctic stratosphere was approximately 3.7 ppbv, but photolytic breakdown into

Table 2. ClO Dimer Formation Rate Constants at 190 K

Source	k_{form} Minus Its Uncertainty	k_{form} Recommended	k_{form} Plus Its Uncertainty
Sander et al. [1989]	5.2E-14	1.2E-13	2.3E-13
Trolier et al. [1990]	8.2E-14	1.0E-13	1.2E-13
Nickolaisen et al. [1994]	8.4E-14	1.0E-13	1.2E-13
JPL 94	6.6E-14	1.1E-13	1.7E-13
This work	8.0E-14	1.1E-13	1.4E-13

Experimental values are extrapolations to 190 K based on the temperature dependence measured over the range of the experiment: Sander et al. [1989] 195-247 K, Trolier et al. [1990] 200-263 K, and Nickolaisen et al. [1994] 195-390 K. Read 5.2E-14 as 5.2×10^{-14} .

Table 3. ClO Dimer Equilibrium Constants at 190 K

Source	k_{eq} Minus Its Uncertainty	k_{eq} Recommended	k_{eq} Plus Its Uncertainty
<i>Cox and Hayman</i> [1988]	7.0E-10	6.2E-8	5.4E-06
<i>Nickolaisen et al.</i> [1994]	1.5E-08	1.8E-7	2.1E-06
JPL 94	1.4E-09	1.3E-7	1.1E-05
This work	1.9E-08	1.3E-7	3.3E-06

Experimental values are extrapolations based on the temperature dependence measured over the range of the experiment: *Cox and Hayman* [1988] 203–300 K, *Nickolaisen et al.* [1994] 260–310 K. The Nickolaisen experiment actually measured the ClO dimer formation and dissociation rate constants, from which the equilibrium constant was derived over the given temperature range (which is limited compared to the formation rate constant data by the dissociation measurements). We have shown equilibrium constant ranges as opposed to dissociation rate constants to allow us to include the Cox and Hayman data. Read 7.0E-10 as 7.0×10^{-10} .

inorganic chlorine is less than complete in the lower stratosphere, even after polar subsidence. Measurements taken within the northern polar vortex during the 1992 winter showed maximum Cl_y values of ~3.1–3.2 ppbv near 20-km altitude [*Woodbridge et al.*, 1995; *von Clarmann et al.*, 1995]. The 3.1 ppbv ClO + Cl_2O_2 calculated using the recommended rate constants and photolysis cross sections therefore requires virtually a complete activation of inorganic chlorine. Use of the high Cl_2O_2 thermal dissociation rate results in an implausibly large value of 5.2 ppbv for total active chlorine.

The use of the newly measured Cl_2O_2 photolysis cross sections [*Huder and DeMore*, 1995] instead of the JPL 94 values results in a significantly larger amount of chlorine present in the dimer, in equilibrium with the observed amounts of ClO, as these cross sections are smaller than the JPL 94 cross sections. The total amount of chlorine in ClO and Cl_2O_2 using the Huder and DeMore cross sections, along with the JPL 94 recommendations for the Cl_2O_2 rate constants, is 4.0 ppbv, as shown in Table 4 (this value becomes at most several tenths lower (~3.5 ppbv) if we push the Cl_2O_2 thermal dissociation rate constant to the lower bound derived here). Even with a slightly lower Cl_2O_2 thermal dissociation rate constant, this value remains greater than the available inorganic chlorine, or even the total chlorine in the Antarctic spring lower stratosphere.

Ozone Depletion as a Function of Time

The ozone loss rate due to the ClO dimer catalytic cycle is given by

$$\frac{d[\text{O}_3]}{dt} = -2k_2[\text{ClO}]^2[\text{M}] \left\{ \frac{J_3}{J_3 + k_{2R}} \right\}$$

where k_{2R} is the dimer thermal dissociation rate constant, the reverse rate of reaction (2), and [M] is the background number density [*Murphy*, 1991]. The term in braces represents the fraction of Cl_2O_2 which photodissociates and

participates in the catalytic cycle out of the total amount of Cl_2O_2 which either photodissociates or undergoes thermal dissociation. For typical temperatures encountered in the Antarctic spring lower stratosphere, this term is near unity once the sun has risen, since the photolysis rate is much larger than the thermal dissociation rate. The uncertainty in the chlorine-catalyzed ozone loss rate is therefore primarily dependent on the uncertainties in the dimer formation rate and the concentration of ClO. Given a typical uncertainty of ~12% in our measurements [*de Zafra et al.*, 1995], the uncertainty in the ozone loss rate can be reduced from +55%/–42% at 186–196 K using the JPL 94 dimer formation rate constant uncertainties, to a significantly smaller range, $\pm 30\%$, using our formation rate constant uncertainties. Here the uncertainties of the dimer formation rate constant and the measurement have been added in quadrature.

We proceed here to use our photochemical model to calculate chemical ozone loss rates based on our observed ClO profiles. Similar calculations have been performed by others [*Solomon*, 1990] based on our earlier data [*Barrett et al.*, 1988], while the loss rate calculated in early September 1993 was shown in our previous comparison of Arctic and Antarctic calculated ozone loss rates [*Shindell et al.*, 1994]. We derive the loss rate by explicitly solving the time dependent differential equation for ozone. Ozone depletion is primarily due to the chlorine catalytic cycle in the Antarctic spring lower stratosphere, but also includes a contribution from bromine chemistry which is ~25% that due to the ClO dimer catalytic cycle.

We have modeled ozone depletion as a function of time using the JPL 94 recommended reaction rate constants and photolysis cross sections along with our ClO measurements. We calculate an increase in the 10–24 km column chemical ozone loss rate from 1.9 ± 0.6 DU/d on September 6, to 3.5 ± 1.1 DU/d on September 19, and to 5.7 ± 1.7 DU/d on October 1, where the uncertainties reflect the 30% value derived from our new constraints on the ClO dimer formation rate constant and our measurement uncertainties. Only about 10% of the

Table 4. Midday Chlorine Abundances

Cl ₂ O ₂ Thermal Dissociation Rate Constant	Cl ₂ O ₂ Photolysis Cross Sections	ClO Mixing Ratio	Cl ₂ O ₂ Mixing Ratio	Total Cl in ClO and Cl ₂ O ₂ (ClO+2×Cl ₂ O ₂)
JPL 94 low	JPL 94 rec	1.9	0.34	2.6
JPL 94 rec	JPL 94 rec	1.9	0.58	3.1
JPL 94 high	JPL 94 rec	2.8	1.2	5.2
JPL 94 rec	Huder and DeMore	1.9	1.0	4.0

For the JPL 94 values, "low" refers to the recommended value minus its uncertainty, "rec" to the recommended value, and "high" to the recommended value plus its uncertainty, all calculated using the values given for the Cl₂O₂ equilibrium and formation rate constants and uncertainties. "Huder and DeMore" refers to their cross-section measurements of 1995. Values in the individual columns may not sum to the total due to rounding. Note as well that the ClO mixing ratios are only accurate to one decimal place, but that the value derived using the JPL low value was actually slightly smaller than that derived using the JPL rec value. The total available inorganic chlorine in the polar lower stratosphere is believed to be about 3.1 ppbv. Values are in units of ppbv.

uncertainty is random, since the considerable uncertainty due to the ClO dimer formation rate constant is purely systematic, so the tripling of the modeled chemical ozone loss rate from early to late September is a statistically significant result. We attribute this increase in chemical ozone loss rates to two causes. (1) The duration of solar exposure during the midday period, defined here as from 2 hours after sunrise to 1 hour before sunset, when ClO is near its maximum abundance (see Figures 2 and 4), lengthens from 7.9 hours on September 6 to 14.3 hours on October 1 at 20 km altitude. (2) The increasing pressure resulting from descent leads to an increase in the rate limiting three-body ClO dimer formation reaction. (Dimer formation, ClO+ClO+M, and therefore the ozone loss rate, increases as the cube of the pressure for a constant ClO mixing ratio, since concentration is proportional to mixing ratio times background pressure.)

To examine the overall effect of the observed descent of ClO more fully, we have included vertical descent at rates of 50-100 m/d in the model, which represent reasonable bounds on the observed descent of the lower stratospheric ClO layer through September [de Zafra *et al.*, 1995]. These descent rates are also in rough agreement with those predicted by the models of Manney *et al.* [1994] and Rosenfield *et al.* [1994], for this time period and location. An acceleration of chemical ozone depletion takes place as stated above, but is now largely masked by the downward vertical transport of air containing larger mixing ratios of ozone into the 10-24 km column. The net effect of the increasing chemical destruction of ozone and the addition of ozone by transport at descent rates in the 50-100 m/d range is an approximately linear rate of ozone depletion in the 10-24 km column throughout September in this simple model simulation.

Figure 7 displays the mixing ratios of ozone, ClO, and reservoir chlorine species at 20-km altitude during an extended 40-day model run which included a relatively conservative descent rate of 50 m/d. Temperatures in the model were set in accordance with the trends seen in

National Meteorological Center (NMC) data for McMurdo [see de Zafra *et al.*, 1995], permitting the existence of NAT PSCs through ~September 30. Here we have had the air parcel encounter a minimal 2 μm²/cm³ surface area PSC

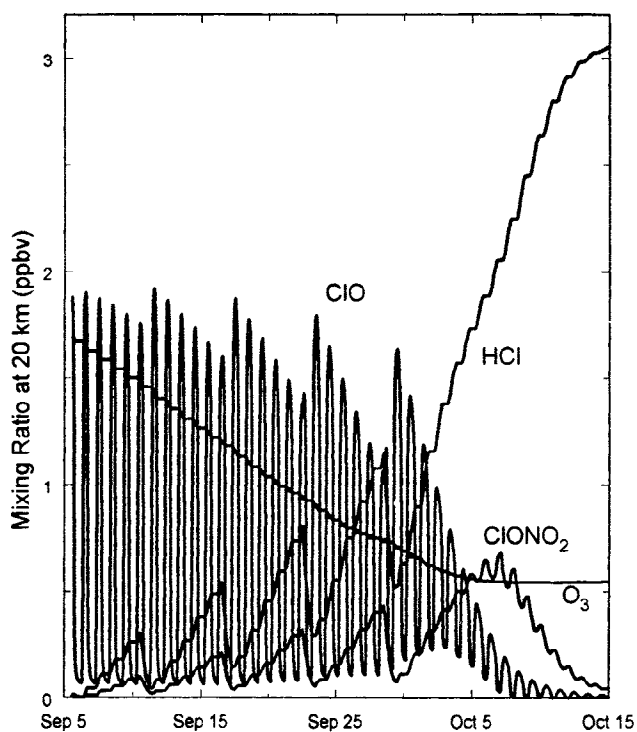


Figure 7. Mixing ratios of ozone, ClO, and the reservoir species HCl and ClONO₂ at 20-km altitude in a model run which included a descent rate of 50 m/d at this altitude. The air parcel encountered a PSC every 6 days through September 30, causing the cyclic pattern of heterogeneous processing seen here. Mixing ratios are in parts per billion by volume for chlorine species, and parts per million by volume for ozone. See text for discussion of temperature variations and PSC surface area during the time period shown here.

every 6 days until September 30, in keeping with observations of sparse PSC activity over McMurdo during this period of 1993. We find that this cyclic heterogeneous activation of chlorine balances out most of the effect of homogeneous deactivation occurring through methane and hydroxyl reactions with chlorine. The slow overall decrease in the abundance of midday ClO and increase in the reservoir species HCl and ClONO₂ at 20 km up to ~September 30 in this model run result partially from descent, rather than indicating purely chemical deactivation of chlorine during this period. A small increase in assumed average surface area or frequency of PSC encounters would prevent even the relatively small transfer to reservoir species during September that is seen in Figure 7. The removal of all PSC processing at the end of September (in accord with rapidly rising temperatures at this time) stopped chlorine activation through heterogeneous chemistry, with the result that chlorine returned rapidly to its reservoirs in October, as shown in Figure 7.

The apparent ozone loss is now essentially linear with time at a given altitude. The loss rate calculated from the model run in Figure 7 is ~1.0 DU/d for the month of September in the 18-20 km region, in quantitative agreement with the apparent linear loss rate seen in the ozonesonde measurements taken at McMurdo Station by the University of Wyoming [Johnson *et al.*, 1995]. For the entire 10-24 km column, the University of Wyoming data again show a linear loss rate for the month of September of 4.1 DU/d. This rate agrees rather well with our model, which for the entire 10-24 km column yields an approximately linear chemistry-plus-transport ozone loss rate of 3.1-4.3 DU/d, depending on descent rates chosen between 50 and 100 m/d.

Summary

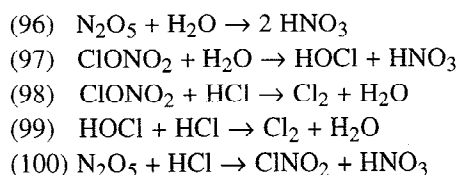
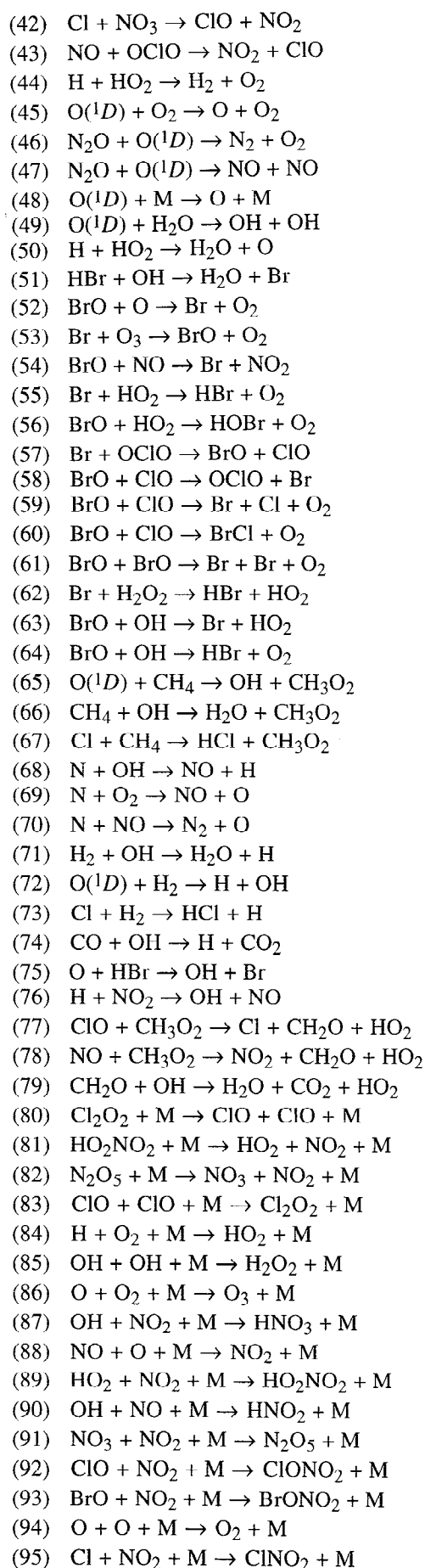
We have compared our observations of diurnal change in chlorine monoxide with a short time-step photochemical model to examine chlorine catalytic chemistry on a diurnal basis in the Antarctic lower stratosphere. We have shown that the reaction rate constants recommended in the 1994 JPL evaluation yield a modeled diurnal behavior of ClO which agrees extremely well with our observations. This short-term diurnal comparison is a critical test of the chemistry which causes longer-term ozone depletion over Antarctica during the austral spring. In addition, we have been able to test the limits on variation for two of the crucial reaction rate constants in the chlorine monoxide dimer catalytic cycle, the ClO dimer formation rate constant and the equilibrium constant between ClO dimer formation and thermal dissociation, which maintain agreement with our diurnal data. Based on this comparison, we have reduced the uncertainty of the ClO dimer formation rate constant by ~40% and reduced the uncertainty of the equilibrium constant by ~60% at 186-196 K compared to the uncertainty ranges given in the JPL 1994 evaluation. The new constraint on the formation rate constant reduces the uncertainty in chlorine catalyzed ozone loss rates

calculated from measured ClO concentrations by ~40% at 186-196 K, significantly improving quantitative comparisons of observed ozone loss with loss rates calculated from observed ClO concentrations. A 40-day model run that includes a small amount of heterogeneous processing through September, along with a realistic rate of downward transport, gives results in good agreement with the total quantity and the linear trend of ozone loss seen in coincident balloon measurements.

Appendix

Chemical Reactions Included in the Model

- (1) $\text{Cl} + \text{O}_3 \rightarrow \text{ClO} + \text{O}_2$
- (2) $\text{ClO} + \text{O} \rightarrow \text{Cl} + \text{O}_2$
- (3) $\text{Cl} + \text{OCIO} \rightarrow \text{ClO} + \text{ClO}$
- (4) $\text{ClO} + \text{O}_3 \rightarrow \text{Cl} + \text{O}_2 + \text{O}_2$
- (5) $\text{ClO} + \text{O}_3 \rightarrow \text{OCIO} + \text{O}_2$
- (6) $\text{O} + \text{OCIO} \rightarrow \text{ClO} + \text{O}_2$
- (7) $\text{OH} + \text{Cl}_2 \rightarrow \text{HOCl} + \text{Cl}$
- (8) $\text{OH} + \text{HCl} \rightarrow \text{H}_2\text{O} + \text{Cl}$
- (9) $\text{OH} + \text{HOCl} \rightarrow \text{H}_2\text{O} + \text{ClO}$
- (10) $\text{O} + \text{HCl} \rightarrow \text{OH} + \text{Cl}$
- (11) $\text{O} + \text{HOCl} \rightarrow \text{OH} + \text{ClO}$
- (12) $\text{OCIO} + \text{OH} \rightarrow \text{HOCl} + \text{O}_2$
- (13) $\text{Cl} + \text{HOCl} \rightarrow \text{Cl}_2 + \text{OH}$
- (14) $\text{H} + \text{O}_3 \rightarrow \text{OH} + \text{O}_2$
- (15) $\text{H} + \text{HO}_2 \rightarrow \text{OH} + \text{OH}$
- (16) $\text{O} + \text{OH} \rightarrow \text{O}_2 + \text{H}$
- (17) $\text{O} + \text{HO}_2 \rightarrow \text{OH} + \text{O}_2$
- (18) $\text{O} + \text{H}_2\text{O}_2 \rightarrow \text{OH} + \text{HO}_2$
- (19) $\text{OH} + \text{HO}_2 \rightarrow \text{H}_2\text{O} + \text{O}_2$
- (20) $\text{OH} + \text{O}_3 \rightarrow \text{HO}_2 + \text{O}_2$
- (21) $\text{OH} + \text{OH} \rightarrow \text{H}_2\text{O} + \text{O}$
- (22) $\text{OH} + \text{H}_2\text{O}_2 \rightarrow \text{H}_2\text{O} + \text{HO}_2$
- (23) $\text{Cl} + \text{H}_2\text{O}_2 \rightarrow \text{HCl} + \text{HO}_2$
- (24) $\text{Cl} + \text{HO}_2 \rightarrow \text{HCl} + \text{O}_2$
- (25) $\text{Cl} + \text{HO}_2 \rightarrow \text{OH} + \text{ClO}$
- (26) $\text{O} + \text{O}_3 \rightarrow \text{O}_2 + \text{O}_2$
- (27) $\text{HO}_2 + \text{O}_3 \rightarrow \text{OH} + \text{O}_2 + \text{O}_2$
- (28) $\text{HO}_2 + \text{HO}_2 \rightarrow \text{H}_2\text{O}_2 + \text{O}_2$
- (29) $\text{ClO} + \text{OH} \rightarrow \text{HO}_2 + \text{Cl}$
- (30) $\text{ClO} + \text{OH} \rightarrow \text{HCl} + \text{O}_2$
- (31) $\text{ClO} + \text{HO}_2 \rightarrow \text{HOCl} + \text{O}_2$
- (32) $\text{O}_3 + \text{NO} \rightarrow \text{NO}_2 + \text{O}_2$
- (33) $\text{O} + \text{NO}_2 \rightarrow \text{O}_2 + \text{NO}$
- (34) $\text{OH} + \text{HNO}_3 \rightarrow \text{H}_2\text{O} + \text{NO}_3$
- (35) $\text{HO}_2 + \text{NO} \rightarrow \text{OH} + \text{NO}_2$
- (36) $\text{NO}_2 + \text{O}_3 \rightarrow \text{NO}_3 + \text{O}_2$
- (37) $\text{NO}_3 + \text{NO} \rightarrow \text{NO}_2 + \text{NO}_2$
- (38) $\text{O} + \text{NO}_3 \rightarrow \text{O}_2 + \text{NO}_2$
- (39) $\text{OH} + \text{HO}_2\text{NO}_2 \rightarrow \text{H}_2\text{O} + \text{NO}_2 + \text{O}_2$
- (40) $\text{ClO} + \text{NO} \rightarrow \text{NO}_2 + \text{Cl}$
- (41) $\text{ClONO}_2 + \text{O} \rightarrow \text{ClO} + \text{NO}_3$



Rate constants have been taken from the 1994 JPL evaluation [DeMore *et al.*, 1994], with the exception of the following reactions:

- (29) and (30): Branching ratio suggested by Chandra *et al.* [1993].
 (46) and (47): Branching ratio measured by Cantrell *et al.* [1994].
 (63): BrO + OH rate constant taken to be analogous to ClO + OH reaction.
 (68): Rate constant given by Atkinson *et al.* [1989].
 (94): Pressure dependent rate constant given by Brasseur and Solomon [1984].
 (96) and (97): Heterogeneous reactions on NAT PSCs and aerosol surfaces (see text).
 (98)-(100): Heterogeneous reactions on NAT PSCs only (see text).

Note that the following reaction steps are assumed to take place instantaneously as the lifetimes of ClOO, CH₃, CH₃O, and HCO are less than a single time step under stratospheric conditions.

- (4), (59), and (77): $\text{ClOO} \rightarrow \text{Cl} + \text{O}_2$.
 (65)-(67): $\text{CH}_3 + \text{O}_2 + \text{M} \rightarrow \text{CH}_3\text{O}_2 + \text{M}$.
 (77) and (78): $\text{O}_2 + \text{CH}_3\text{O} \rightarrow \text{CH}_2\text{O} + \text{HO}_2$.
 (79): $\text{HCO} + \text{O}_2 \rightarrow \text{HO}_2 + \text{CO}$.

Photolysis Reactions Included in the Model

- (1) $\text{ClO} + h\nu \rightarrow \text{Cl} + \text{O}$
 (2) $\text{Cl}_2 + h\nu \rightarrow \text{Cl} + \text{Cl}$
 (3) $\text{OCIO} + h\nu \rightarrow \text{O} + \text{ClO}$
 (4) $\text{Cl}_2\text{O}_2 + h\nu \rightarrow \text{Cl} + \text{Cl} + \text{O}_2$
 (5) $\text{HCl} + h\nu \rightarrow \text{H} + \text{Cl}$
 (6) $\text{HOCl} + h\nu \rightarrow \text{OH} + \text{Cl}$
 (7) $\text{H}_2\text{O}_2 + h\nu \rightarrow \text{OH} + \text{OH}$
 (8) $\text{HO}_2\text{NO}_2 + h\nu \rightarrow \text{HO}_2 + \text{NO}_2$
 (9) $\text{HO}_2\text{NO}_2 + h\nu \rightarrow \text{OH} + \text{NO}_3$
 (10) $\text{N}_2\text{O}_5 + h\nu \rightarrow \text{NO}_3 + \text{NO}_2$
 (11) $\text{HNO}_3 + h\nu \rightarrow \text{OH} + \text{NO}_2$
 (12) $\text{NO}_2 + h\nu \rightarrow \text{NO} + \text{O}$
 (13) $\text{NO}_3 + h\nu \rightarrow \text{NO}_2 + \text{O}$
 (14) $\text{NO}_3 + h\nu \rightarrow \text{NO} + \text{O}_2$
 (15) $\text{ClONO}_2 + h\nu \rightarrow \text{Cl} + \text{NO}_3$
 (16) $\text{ClONO}_2 + h\nu \rightarrow \text{O} + \text{ClNO}_2$
 (17) $\text{N}_2\text{O} + h\nu \rightarrow \text{N}_2 + \text{O}(^1D)$
 (18) $\text{O}_3 + h\nu \rightarrow \text{O}(^1D) + \text{O}_2$
 (19) $\text{O}_3 + h\nu \rightarrow \text{O} + \text{O}_2$
 (20) $\text{BrONO}_2 + h\nu \rightarrow \text{BrO} + \text{NO}_2$
 (21) $\text{BrCl} + h\nu \rightarrow \text{Br} + \text{Cl}$
 (22) $\text{HOBr} + h\nu \rightarrow \text{Br} + \text{OH}$
 (23) $\text{BrO} + h\nu \rightarrow \text{Br} + \text{O}$
 (24) $\text{HBr} + h\nu \rightarrow \text{Br} + \text{H}$
 (25) $\text{CO}_2 + h\nu \rightarrow \text{CO} + \text{O}$
 (26) $\text{ClNO}_2 + h\nu \rightarrow \text{Cl} + \text{NO}_2$

- (27) $\text{CH}_2\text{O} + h\nu \rightarrow \text{H} + \text{HO}_2 + \text{CO}$
 (28) $\text{CH}_2\text{O} + h\nu \rightarrow \text{H}_2 + \text{CO}$
 (29) $\text{H}_2\text{O} + h\nu \rightarrow \text{H} + \text{OH}$
 (30) $\text{NO} + h\nu \rightarrow \text{N} + \text{O}$
 (31) $\text{O}_2 + h\nu \rightarrow \text{O} + \text{O}$

Photolysis cross sections have been taken from the 1994 JPL evaluation [DeMore *et al.*, 1994], with the exception of the following reactions:

- (13) and (14): Cross sections given by Wayne *et al.* [1991].
 (21): Taken to be analogous to Cl_2 cross sections.
 (22): Cross sections of HOCl used, but shifted up 30 nm as given by Atkinson *et al.* [1992].
 (24): Taken to be analogous to HCl cross sections.
 (25): Cross sections given by Hudson and Kieffer [1975].
 (29): Parameterization of Schumann-Runge band cross sections given by Nicolet [1984].
 (30): Parameterization of Schumann-Runge band cross sections given by Nicolet and Cieslik [1980].
 (31): Parameterization of Schumann-Runge band cross sections given by Nicolet *et al.* [1989].

Note also that in reaction (4), $\text{ClOO} \rightarrow \text{Cl} + \text{O}_2$ instantaneously.

Acknowledgments. J. M. Reeves participated in field measurements of data used here. We are grateful to V. Dvortsov for his generous assistance with the radiation code. We thank B. Johnson and T. Deshler of the University of Wyoming for providing us with their data before publication, as well as J. Mergenthaler, A. Roche, J. Russell III, and J. Waters for allowing us access to their UARS data. We also thank R. Garcia, D. Weisenstein, and L. Perliski for helpful advice on modeling, and we wish to acknowledge two anonymous referees whose suggestions were appreciated. This work was supported by NASA under grants NAGW-2182 and NAG-1-1354 and by the NSF Office of Polar Programs under grant DPP8922688.

References

- Atkinson, R., D. L. Baulch, R. A. Cox, R. F. Hampson Jr., J. A. Kerr, and J. Troe, Evaluated kinetic and photochemical data for atmospheric chemistry supplement IV, *J. Phys. Chem. Ref. Data*, *21*, 1125-1568, 1992.
- Atkinson, R., D. L. Baulch, R. A. Cox, R. F. Hampson Jr., J. A. Kerr, and J. Troe, IUPAC subcommittee on gas kinetic data evaluation for atmospheric chemistry, *J. Phys. Chem. Ref. Data*, *18*, 881-1097, 1989.
- Barrett, J. W., P. M. Solomon, R. L. de Zafra, M. Jaramillo, L. Emmons, and A. Parrish, Formation of the Antarctic ozone hole by the ClO dimer mechanism, *Nature*, *336*, 455-458, 1988.
- Brasseur, G., and S. Solomon, *Aeronomy of the Middle Atmosphere*, D. Reidel, Norwell, Mass., 1986.
- Briegleb, B. P., Delta-Eddington approximation for solar radiation in the NCAR community climate model, *J. Geophys. Res.*, *97*, 7603-7612, 1992.
- Brune, W. H., J. G. Anderson, and K. R. Chan, In situ observations of BrO over Antarctica: ER-2 aircraft results from 54 S to 72 S latitude, *J. Geophys. Res.*, *94*, 16,639-16,647, 1989.
- Cantrell, C. A., R. E. Shetter, and J. G. Calvert, Branching ratios for the $\text{O}(^1D) + \text{N}_2\text{O}$ reaction, *J. Geophys. Res.*, *99*, 3739-3743, 1994.
- Chandra, S., C. H. Jackman, A. R. Douglass, E. L. Fleming, and D. B. Considine, Chlorine catalyzed destruction of ozone: Implications for ozone variability in the upper stratosphere, *Geophys. Res. Lett.*, *20*, 351-354, 1993.
- Cox, R. A., and G. D. Hayman, The stability and photochemistry of dimers of the ClO radical and implications for Antarctic ozone depletion, *Nature*, *332*, 796-800, 1988.
- Crutzen, P. J., R. Müller, C. Brühl and T. Peter, On the potential importance of the gas phase reaction $\text{CH}_3\text{O}_2 + \text{ClO} \rightarrow \text{ClOO} + \text{CH}_3\text{O}$ and the heterogeneous reaction $\text{HOCl} + \text{HCl} \rightarrow \text{H}_2\text{O} + \text{Cl}_2$, *Geophys. Res. Lett.*, *19*, 1113-1116, 1992.
- DeMore, W.B., S. P. Sander, D. M. Golden, R. F. Hampson, M. J. Kurylo, C. J. Howard, A. R. Ravishankara, C. E. Kolb, and M. J. Molina, Chemical kinetics and photochemical data for use in stratospheric modeling, in Evaluation 11, *JPL Publ.*, 94-26, 1994.
- de Zafra, R. L., M. Jaramillo, J. W. Barrett, L. K. Emmons, P. M. Solomon, and A. Parrish, New observations of a large concentration of ClO in the springtime lower stratosphere over Antarctica and its implications for ozone-depleting chemistry, *J. Geophys. Res.*, *94*, 11,423-11,428, 1989.
- de Zafra, R. L., W. H. Mallison, M. Jaramillo, J. M. Reeves, L. K. Emmons, and D. T. Shindell, A new high-sensitivity superconducting receiver for mm-wave remote sensing spectroscopy of the stratosphere, in *Ozone in the Troposphere and Stratosphere, Proceedings of the 1992 Quadrennial Ozone Symposium, NASA Conf. Publ., CP-3266*, 719-722, 1994.
- de Zafra, R. L., J. M. Reeves, and D. T. Shindell, Chlorine monoxide in the Antarctic spring vortex over McMurdo Station, 1993, I, Evolution of midday vertical profiles, *J. Geophys. Res.*, *100*, 13,999-14,008, 1995.
- Dvortsov, V.L., S.G. Zvenigorodsky, and S.P. Smyslaev, On the use of Isaksen-Luther method of computing photodissociation rates in photochemical models, *J. Geophys. Res.*, *97*, 7593-7601, 1992.
- Hofmann, D. J., and T. Deshler, Stratospheric cloud observations during formation of the Antarctic ozone hole in 1989, *J. Geophys. Res.*, *96*, 2897-2912, 1991.
- Huder, K. J., and W. B. DeMore, Absorption cross sections of the ClO dimer, *J. Phys. Chem.*, *99*, 3905-3910, 1995.
- Hudson, R. D., and L. J. Kieffer, The natural stratosphere of 1974, *CIAP Monogr.*, Vol. 1, 1975.
- Johnson, B. J., T. Deshler, and R. Zhao, Ozone profiles at McMurdo Station, Antarctica, during the spring of 1993: Record low ozone season, *Geophys. Res. Lett.*, *22*, 183-186, 1995.
- Lefèvre, F., G. P. Brasseur, I. Folkins, A. K. Smith, and P. Simon, Chemistry of the 1991-1992 stratospheric

- winter: Three-dimensional model simulations, *J. Geophys. Res.*, *99*, 8183-8195, 1994.
- López-Valverde, M. A., M. López-Puertas, C. J. Marks, and F. W. Taylor, Global and seasonal variations in middle atmosphere CO from UARS/ISAMS, *Geophys. Res. Lett.*, *20*, 1247-1250, 1993.
- Manney, G. L., R. L. Zurek, A. O'Neill, and R. Swinbank, On the motion of air through the stratospheric polar vortex, *J. Atmos. Sci.*, *51*, 2973-2994, 1994.
- Molina, L. T., and M. J. Molina, Production of Cl₂O₂ from the self-reaction of the ClO radical, *J. Phys. Chem.*, *91*, 433-436, 1987.
- Murphy, D. M., Ozone loss rates calculated along ER-2 flight tracks, *J. Geophys. Res.*, *96*, 5045-5053, 1991.
- Nicolaisen, S. L., R. R. Friedl, and S. P. Sander, Kinetics and mechanism of the ClO + ClO reaction: Pressure and temperature dependences of the bimolecular and termolecular channels and thermal decomposition of chlorine peroxide, *J. Phys. Chem.*, *98*, 155-169, 1994.
- Nicolet, M., On the photodissociation of water vapour in the mesosphere, *Planet. Space Sci.*, *32*, 871-880, 1984.
- Nicolet, M., and S. Cieslik, The photodissociation of nitric oxide in the mesosphere and stratosphere, *Planet. Space Sci.*, *28*, 105-115, 1980.
- Nicolet, M., S. Cieslik, and R. Kennes, Aeronomic problems of molecular oxygen photodissociation, V, Predissociation in the Schumann-Runge bands of oxygen, *Planet. Space Sci.*, *37*, 427-458, 1989.
- Rodriguez, J. M., et al., Nitrogen and chlorine species in the spring Antarctic stratosphere: Comparison of models with Airborne Antarctic Ozone Experiment observations, *J. Geophys. Res.*, *94*, 16,683-16,703, 1989.
- Rosenfield, J. E., P. A. Newman, and M. R. Schoeberl, Computations of diabatic descent in the stratospheric polar vortex, *J. Geophys. Res.*, *99*, 16,677-16,690, 1994.
- Sander, S. P., R. P. Friedl, and Y. L. Yung, Rate for formation of the ClO dimer in the polar stratosphere: implications for ozone loss, *Science*, *245*, 1095-1098, 1989.
- Schmidt, U., and A. Khedim, In situ measurements of carbon dioxide in the winter arctic vortex and at midlatitudes: An indicator of the "age" of stratospheric air, *Geophys. Res. Lett.*, *18*, 763-766, 1991.
- Shindell, D. T., J. M. Reeves, L. K. Emmons, and R. L. de Zafra, Arctic chlorine monoxide observations during spring 1993 over Thule, Greenland, and implications for ozone depletion, *J. Geophys. Res.*, *99*, 25,697-25,704, 1994.
- Solomon, S., Progress towards a quantitative understanding of Antarctic ozone depletion, *Nature*, *347*, 347-354, 1990.
- Toon, O. B., C. P. McKay, T. P. Ackerman, and K. Santhanam, Rapid calculation of radiative heating rates and photodissociation rates in inhomogeneous multiple scattering atmospheres, *J. Geophys. Res.*, *94*, 16,287-16,290, 1989.
- Trolier, M., R. L. Mauldin III, and A. R. Ravishankara, Rate coefficient for the termolecular channel of the self-reaction of ClO, *J. Phys. Chem.*, *94*, 4896-4907, 1990.
- Turco, R. P., O. B. Toon, and P. Hamill, Heterogeneous physicochemistry of the polar ozone hole, *J. Geophys. Res.*, *94*, 16,493-16,510, 1989.
- von Clarmann, T., et al., Determination of the stratospheric chlorine budget in the spring arctic vortex from MIPAS B limb emission spectra and air sampling experiments, *J. Geophys. Res.*, *100*, 13,979-13,997, 1995.
- Wayne, R. P., et al., The nitrate radical: Physics, chemistry, and the atmosphere, *Atmos. Environ. A*, *25A*, 1-203, 1991.
- Woodbridge, E. L., et al., Estimates of total organic and inorganic chlorine in the lower stratosphere from in situ and flask measurements during AASE II, *J. Geophys. Res.*, *100*, 3057-3064, 1995.
- World Meteorological Organization, Atmospheric ozone, *Rep. 16*, Global Ozone Res. and Monitoring Proj., Geneva, 1985.
- World Meteorological Organization, Scientific assessment of ozone depletion, *Rep. 25*, Global Ozone Res. and Monitoring Proj., Geneva, 1991.

R. L. de Zafra, Physics Department, State University of New York at Stony Brook, Stony Brook, NY 11794.

D. T. Shindell, NASA GISS/Columbia University, 2880 Broadway, New York, NY 10025. (email: dshindel@thebes.giss.nasa.gov)

(Received August 24, 1994; revised September 26, 1995; accepted October 13, 1995.)